EJN European Journal of Neuroscience

FENS Federation of European Neuroscience Societies

European Journal of Neuroscience, Vol. 41, pp. 398–409, 2015 doi:10.1111/ejn.12799

MOLECULAR AND SYNAPTIC MECHANISMS

Synaptic vesicle glycoprotein 2A modulates vesicular release and calcium channel function at peripheral sympathetic synapses

Christian Vogl,[1]* Shota Tanifuji,[2] Benedicte Danis,[3] Veronique Daniels,[3] Patrik Foerch,[3] Christian Wolff,[3] Benjamin J. Whalley,[1] Sumiko Mochida[2] and Gary J. Stephens[1]
[1]School of Pharmacy, University of Reading, Reading, UK
[2]Department of Physiology, Tokyo Medical University, Tokyo, Japan
[3]UCB Centre for CNS Innovation, UCB Pharma SA, Braine l'Alleud, Belgium

Keywords: Cav2.2, cholinergic, rat, synaptic transmission

Abstract

Synaptic vesicle glycoprotein (SV)2A is a transmembrane protein found in secretory vesicles and is critical for Ca^{2+}-dependent exocytosis in central neurons, although its mechanism of action remains uncertain. Previous studies have proposed, variously, a role of SV2 in the maintenance and formation of the readily releasable pool (RRP) or in the regulation of Ca^{2+} responsiveness of primed vesicles. Such previous studies have typically used genetic approaches to ablate SV2 levels; here, we used a strategy involving small interference RNA (siRNA) injection to knockdown solely presynaptic SV2A levels in rat superior cervical ganglion (SCG) neuron synapses. Moreover, we investigated the effects of SV2A knockdown on voltage-dependent Ca^{2+} channel (VDCC) function in SCG neurons. Thus, we extended the studies of SV2A mechanisms by investigating the effects on vesicular transmitter release and VDCC function in peripheral sympathetic neurons. We first demonstrated an siRNA-mediated SV2A knockdown. We showed that this SV2A knockdown markedly affected presynaptic function, causing an attenuated RRP size, increased paired-pulse depression and delayed RRP recovery after stimulus-dependent depletion. We further demonstrated that the SV2A–siRNA-mediated effects on vesicular release were accompanied by a reduction in VDCC current density in isolated SCG neurons. Together, our data showed that SV2A is required for correct transmitter release at sympathetic neurons. Mechanistically, we demonstrated that presynaptic SV2A: (i) acted to direct normal synaptic transmission by maintaining RRP size, (ii) had a facilitatory role in recovery from synaptic depression, and that (iii) SV2A deficits were associated with aberrant Ca^{2+} current density, which may contribute to the secretory phenotype in sympathetic peripheral neurons.

Introduction

Synaptic vesicle glycoprotein (SV)2A is the major 12-transmembrane domain glycoprotein SV2 family isoform and is critical for regulated exocytosis (Buckley & Kelly, 1985; Bajjalieh *et al.*, 1992; Feany *et al.*, 1992). It is the protein target for the antiepileptic drug levetiracetam and its analogues (Lynch *et al.*, 2004; De Smedt *et al.*, 2007; Daniels *et al.*, 2013), and botulinum and tetanus neurotoxins (Dong *et al.*, 2006; Yeh *et al.*, 2010). Genetic deletion of SV2A causes a reduction in stimuli-evoked transmitter release and produces a phenotype characterised by severe seizures in mice and, as a consequence, a severely restricted lifespan (Crowder *et al.*, 1999; Janz *et al.*, 1999). Interestingly, it was reported that overexpression of SV2A also reduced evoked neurotransmitter release (Iezzi *et al.*, 2005; Nowack *et al.*, 2011). These studies highlight the importance of SV2A in the maintenance of regulated neurotransmission. Despite this knowledge, the exact mechanism of SV2 action at the presynapse remains controversial. Previous studies have proposed a role of SV2 in vesicle pool regulation in central and retinal neurons and neuroendocrine cells (Xu & Bajjalieh, 2001; Iezzi *et al.*, 2005; Custer *et al.*, 2006; Wan *et al.*, 2010), although others failed to observe similar effects and have suggested that SV2 renders primed vesicles Ca^{2+}-responsive for release (Chang & Sudhof, 2009). In particular, the effects of SV2A on the regulation of presynaptic Ca^{2+} concentration are controversial (Mendoza-Torreblanca *et al.*, 2013). For example, although SV2A-deficient hippocampal neurons were reported to show normal electrophysiological responses, repetitive stimulation in SV2A/SV2B-deleted neurons increased synaptic transmission in response to trains of action potentials, an effect reversed by the Ca^{2+} chelator, EGTA (Janz *et al.*, 1999; Chang & Sudhof, 2009). Similarly, in rod bipolar cells, deletion of the predominant SV2B isoform caused presynaptic Ca^{2+} accumulation and changes to synaptic function (Wan *et al.*, 2010),

Correspondence: Gary J. Stephens, as above.
E-mail: g.j.stephens@reading.ac.uk

S.M. and G.J.S. contributed equally to this work.

**Present address*: Department of Otolaryngology, University of Goettingen Medical Center, Goettingen, D-37075, Germany

Received 24 June 2014, revised 3 November 2014, accepted 5 November 2014

although SV2B knockouts do not have any obvious phenotype. We have recently shown that the SV2A ligand, levetiracetam, inhibits presynaptic voltage-dependent Ca^{2+} channels (VDCCs) through an intracellular pathway in superior cervical ganglion (SCG) neurons (Vogl *et al.*, 2012), suggesting a potential SV2A role in VDCC modulation. SV2A has also been associated with the modulation of VDCC-binding partners, including synaptotagmin, the Ca^{2+} sensor for synaptic release in neurons. Thus, SV2A binds synaptotagmin (Schivell *et al.*, 1996), mediates synaptotagmin trafficking (Yao *et al.*, 2010) and, in SCG synapses, introduction of an SV2A amino terminal peptide (to disrupt known SV2A–synaptotagmin interaction sites) inhibits transmitter release (Schivell *et al.*, 2005).

To address these issues, we took advantage of the SCG synapse preparation, an established model to study the role of VDCCs in synaptic function (Mochida *et al.*, 2003; Stephens & Mochida, 2005; Bucci *et al.*, 2011). SCG synapses allow the introduction of exogenous material into a presynaptic locus (Ma & Mochida, 2007); thus, we employed a small interference RNA (siRNA) approach for target-specific and solely presynaptic SV2A knockdown at SCG synapses. We demonstrate that SV2A knockdown is associated with a secretory phenotype, causing deficits in the RRP size and attenuated RRP recovery, which suggests that SV2A normally maintains correct vesicular release in SCG neurons. These effects were also associated with a VDCC phenotype, suggesting that functional modulation of presynaptic VDCCs by SV2A also regulates stimuli-evoked transmission between peripheral neurons.

Materials and methods

Ethical standards

Experiments were conducted in accordance with the UK Animals (Scientific Procedures) Act, 1986. Work was also subject to ethical approval at all centres; thus, the University of Reading Local Ethical Research Panel and the Ethics Committee of Tokyo Medical University approved the work.

Tissue culture

Long-term superior cervical ganglion cultures for microelectrode recordings

The SCG neurons were cultured as previously described (Mochida, 1995). Briefly, Wistar rats (postnatal day 7) were anesthetised with diethylether and decapitated following the guidelines of the Physiological Society of Japan. The SCGs were desheathed, incubated in L-15 medium (Gibco Industries, Inc., Langley, OK, USA) containing 0.5 mg/mL collagenase (Worthington Biochemical Corp., Lakewood, NJ, USA) and gently triturated. After washing, centrifugation and resuspension, isolated neurons were plated and maintained in a water-saturated incubator (37 °C, 5% CO_2) for more than 5 weeks in growth medium that comprised 84% Eagle's minimal essential medium, 10% fetal calf serum, 5% horse serum, 1% penicillin–streptomycin (all from Gibco Industries, Inc.) and nerve growth factor (2.5 S, grade II; Alomone, Jerusalem, Israel). The medium was changed twice per week.

Superior cervical ganglion neurons for patch-clamp recordings

The SCGs were obtained from postnatal day 21-25 male Wistar rats as described previously (Bucci *et al.*, 2011). Briefly, SCGs were dissected and placed in cold L-15 medium (Sigma Aldrich, Poole, UK) containing 5% penicillin–streptomycin (Gibco Invitrogen, Paisley, UK). The ganglia were then acutely dissociated in DMEM (Dulbecco's Modified Eagle's Medium) containing 0.5 mg/mL trypsin, 1 mg/mL collagenase and 3.6 mg/mL glucose (all from Sigma Aldrich). The digestion reaction was stopped by the addition of 84% Eagle's minimal essential medium, 10% fetal calf serum, 5% horse serum (all from Lonza, Wokingham, UK), 25 ng/mL nerve growth factor (2.5 S, grade II; Alomone) and 1% penicillin–streptomycin supplemented with 4 μM aphidicolin (Sigma Aldrich) to inhibit glial proliferation. Cells were plated onto coverslips coated with poly-L-ornithine (Sigma Aldrich) and incubated overnight in a humidified incubator (37 °C, 5% CO_2) before microinjection with either non-silencing RNA (nsRNA) or SV2A-siRNA (both 10 μM in the injection pipette) and fluorescein-dextran or rhodamine B-dextran 10 000 MW (Life Technologies, Paisley, UK) markers. The nsRNA-injected and siRNA-injected coverslips were used in parallel to avoid cell culture-related artifacts. All recordings were performed at 4 days after RNA injection.

tsA201 cell culture and transfection procedure

The tsA201 cells were cultured in DMEM with 10% fetal bovine serum and 1% penicillin–streptomycin. Cells were transiently transfected with $Ca_V2.2$, $\alpha_2\delta_1$, β_{2a} and either pmaxGFP (green fluorescent protein) or pcDNA3.3 SV2A-GFP (kind gift of UCB Pharma, Braine l'Alleud, Belgium) in antibiotic-free growth medium using Fugene 6 (Promega, Southampton, UK). Cells were plated onto coverslips coated with poly-L-ornithine (Sigma Aldrich) and incubated in a humidified incubator (37 °C, 5% CO_2). Electrophysiological recordings were performed at 2 days post-transfection.

In vitro *testing of small interference RNA efficiency*

Synaptic vesicle glycoprotein 2A expression analysis and knockdown efficiency

Stable HEK FLipIn cells overexpressing rat SV2A (Rn-SV2A) were generated (Life Technologies) and stable expression was confirmed by quantitative real-time polymerase chain reaction and Western blotting. Cells were seeded in six-well plates at 1×10^6 cells/well in DMEM without antibiotics and transfected with validated siRNAs (5 μM/well) from two different sources (siRNA 1-4, Sigma Mission® siRNA; siRNA 5-7, Life Technologies Stealth siRNA) using TransIT®-TKO (Mirus Bio, Madison, USA). Cells were harvested at 48 h post-transfection, total cellular RNA extracted (RNeasy Plus Mini Kit, Qiagen, KJ Venlo, Netherlands) and concentrations assessed using a NanoDrop ND-1000 spectrophotometer. Total RNA (500 μg) was used to synthesise cDNA (Applied Biosystems High Capacity cDNA reverse transcription kit, Life Technologies) and TaqMan RT-qPCR reactions were performed (Applied Biosystems 7900HT Sequence Detection System). Undiluted, 10× and 100× diluted cDNA was analysed in duplicate for Rn-SV2A expression using Applied Biosystems TaqMan gene expression assays with β-actin as the housekeeping gene. Cq values were obtained using automatic threshold and baseline methods (Applied Biosystems SDS 2.3 software, Life Technologies). Relative gene expression was calculated using the delta Cq method ($2^{-\Delta CQ}$) (de Kok *et al.*, 2000) (Supporting Information Fig. S1). For all subsequent experiments, siRNA#5 (sequence GCUGCGUCUGAAGUCAGUGUCCUUU), which produced maximum SV2A knockdown in HEK293T cells, was used alongside the recommended High-GC nsRNA (Life Technologies).

Immunofluorescence microscopy

The SCG neurons were washed and fixed with acetone prior to permeabilization with phosphate-buffered saline containing 0.25% Triton X-100. After blocking in phosphate-buffered saline with 0.05% Triton X-100, 1% bovine serum albumin and 2% fetal bovine serum, cells were probed with primary antibodies against SV2A and synaptophysin 1 (both 1 : 1000; Synaptic Systems, Göttingen, Germany), and visualised with fluorophore-conjugated secondary antibodies (Alexa Fluor 488 or 633, both 1 : 1000; Life Technologies) using an AxioImager microscope with Axiovision software (Carl Zeiss Ltd, Welwyn Garden City, UK) or a Leica TCS SP2 confocal laser-scanning microscope equipped with Ar 488 nm and HeNe 633 nm lasers and a 63 × /1.4 NA oil-immersion lens (Leica Microsystems Ltd, Milton Keynes, UK). In parallel, control experiments with primary antibodies omitted were performed to ensure secondary antibody specificity (see Vogl *et al.*, 2012). Images were background-subtracted and adjusted for brightness and contrast with ImageJ (Schneider *et al.*, 2012) for illustration purposes only.

Electrophysiology

Synaptic transmission between superior cervical ganglion neurons

Paired intracellular recordings were made from two proximal neurons in long-term culture using microelectrodes filled with 1 M potassium acetate (70–90 MΩ) as described previously (Ma *et al.*, 2009). Briefly, SCG neurons were superfused with modified Krebs solution containing (in mM): 136 NaCl, 5.9 KCl, 2.5 $CaCl_2$, 1.2 $MgCl_2$, 11 glucose, and 3 Na-HEPES, pH 7.4 (adjusted with NaOH). Action potentials were generated in a neuron by current injection (at 0.1 Hz) through the intracellular recording electrode and excitatory postsynaptic potentials (EPSPs) recorded from the synaptically-coupled neuron. Data were obtained at room temperature (20–22 °C). Data were analysed using software written by the late Ladislav Tauc (CNRS, France).

Whole-cell voltage clamp

Experiments were performed as described previously (Bucci *et al.*, 2011; Vogl *et al.*, 2012). Borosilicate glass capillaries (Harvard Apparatus, Kent, UK) had resistances of 4–6 MΩ when filled with intracellular solution consisting of (in mM): 140 CsCl, 1 EGTA, 1 $MgCl_2$, 0.1 $CaCl_2$, 4 Mg-ATP and 10 HEPES, pH adjusted to 7.3 (CsOH). The extracellular bath solution contained (in mM): 160 tetraethylammonium-bromide, 3 KCl, 1 $NaHCO_3$, 1 $MgCl_2$, 10 HEPES, 4 D-glucose and 2 $CaCl_2$ for SCG neurons, 10 $CaCl_2$ for tsA201 cells, pH 7.4 (Tris base). Membrane currents were acquired at a holding potential (V_H) of -70 mV using an Axopatch 200B patch-clamp amplifier and WINWCP v4.0.7 software (John Dempster, University of Strathclyde, UK). Linear components of capacitive and leak currents were subtracted using the standard P/4 protocol. Series resistance compensation of >70% was typically employed. A liquid junction potential of −21.7 mV was not corrected for. Nifedipine (10 μM) was used to inhibit Ca_V1 VDCCs. All recordings were performed at room temperature (20–22 °C). Data were analysed offline using WINWCP v4.0.7 and ORIGINPRO 7.0 (Microcal, Northampton, MA, USA) software. Current–voltage data were fitted with the equation

$$\text{Current density} : G_{max}(V - V_{rev})/(1 + \exp((V - V_{0.5})/k))$$

where G_{max} is the maximum conductance, V_{rev} is the null potential, $V_{0.5}$ is the voltage at which 50% of the current is activated and k is the slope factor.

Statistical methods

Data are presented as mean ± SD (unless stated) or mean ± SEM and statistical significance was determined by two-sample Student's *t*-tests or ANOVA with posthoc Bonferroni or Dunnett's test as indicated in the text. Statistically significant differences were accepted at $P < 0.05$.

Results

Synaptic vesicle glycoprotein 2A-small interference RNA reduces synaptic vesicle glycoprotein 2A expression in superior cervical ganglion presynaptic terminals

We have previously demonstrated SV2A expression and antibody specificity in cultured SCG neurons (Vogl *et al.*, 2012); here, we first showed that SV2A colocalized with the presynaptic marker synaptophysin 1 at SCG neuronal presynaptic terminals in the long-term cultures used in this study (Fig. 1A). Moreover, antibody specificity was demonstrated in untransfected tsA201 cells, which lack SV2A expression (see Fig. 6Ai). These experiments established SV2A expression at SCG presynaptic terminals. Before assessing siRNA-mediated SV2A knockdown and its functional consequences in SCG neurons, seven siRNAs were screened in a stable HEK293T cell line overexpressing Rn-SV2A (Rn-SV2A HEK293T) and their knockdown efficiencies were measured by quantitative real-time polymerase chain reaction. All investigated siRNAs caused significant knockdown relative to nsRNA treatment or control transfection reagent (TKO) alone, whereas transfection of nsRNA had no effect on SV2A-mRNA levels in this assay (Supporting Information Fig. S1). On average, SV2A-siRNA#5 caused the highest degree of mRNA knockdown in Rn-SV2A HEK293T (Fig. 1B) and was hence used for all subsequent siRNA experiments. To confirm knockdown of SV2A protein in our experiments, selected SCG neurons were cytoplasmically microinjected with SV2A-siRNA alongside a fluorescent indicator dye (i.e. dextran-coupled rhodamine). In these experiments, microinjection of SV2A-siRNA#5 significantly decreased somatic SV2A fluorescence intensity in comparison to non-injected cells (Fig. 1C and D). The observed decrease in SV2A fluorescence intensity, in combination with our HEK293 knockdown experiments, strongly argued for successful SV2A depletion in the injected SCG neurons.

Presynaptic synaptic vesicle glycoprotein 2A knockdown attenuates readily releasable pool size in sympathetic neurons

The above experiments established knockdown of SV2A in SCG neurons. The SCG preparation is a useful model as it permits the injection of exogenous material into the presynaptic partner of synaptically-coupled neurons and allows the investigation of presynaptic effects, such as on vesicular release (Ma & Mochida, 2007). In these cells, cholinergic synapses form between postganglionic neurons in culture (Iacovitti *et al.*, 1981). Thus, we microinjected SV2A-siRNA or control nsRNA into SCG neurons and examined the effects of presynaptic SV2A knockdown at SCG synapses on cholinergic transmission. To investigate SV2A synaptic function, we first subjected nsRNA-injected and SV2A-siRNA-injected SCG neurons to a

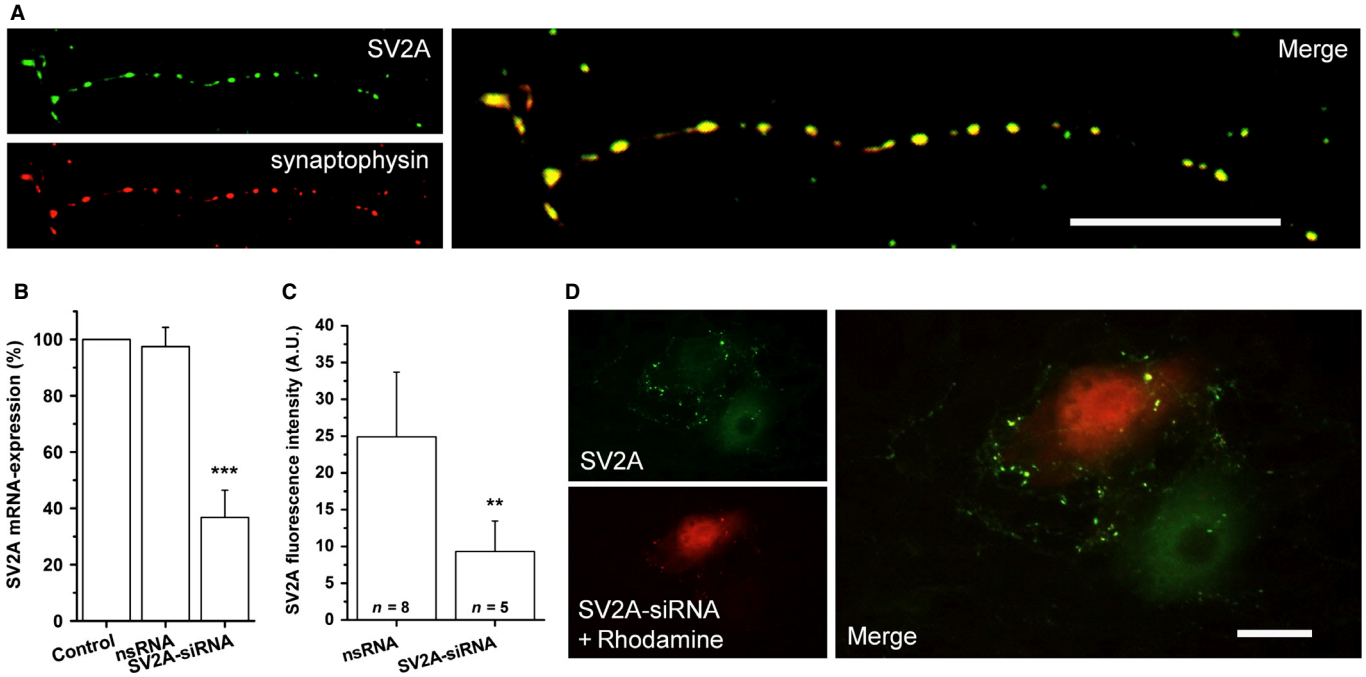

FIG. 1. SV2A expression and knockdown efficiency in SCG neurons and stable Rn-SV2A HEK293T cells. (A) Representative images of SV2A (green), synaptophysin 1 (red) and merged channels illustrate the common presynaptic distribution of the two proteins. (B) SV2A expression analysis of stably expressing Rn-SV2A in HEK293T cells transiently transfected with either nsRNA or SV2A-siRNA. mRNA expression levels were measured by quantitative real-time polymerase chain reaction and normalised to β-actin. Presented are pooled results from four independent experiments expressed as mean ± SD. (C) SV2A fluorescence intensity in SCG neurons. In injected SCG neurons, SV2A-siRNA decreased SV2A fluorescence intensity by ~60% compared with culture-matched injection of nsRNA. (D) Representative immunofluorescence image of SCG neurons coinjected with SV2A-siRNA and rhodamine B-dextran injection marker (red) and an adjacent non-injected cell (green) and merged channels. Note that SV2A fluorescence intensity of SV2A-siRNA-injected neurons is markedly decreased in comparison to adjacent non-injected cells. Scale bars, 20 μm. $^{**}P < 0.01$, Student's one-tailed two-sample *t*-test; $^{***}P < 0.001$, one-way ANOVA followed by a posthoc two-sided Dunnett's test. A.U., arbitrary units.

protocol of a high-frequency train of action potentials (20 Hz, 2 s) to elicit multi-peak EPSPs that depressed quickly before reaching a steady state (Fig. 2A and B). Such protocols allow the investigation of the effects of SV2A knockdown on EPSP amplitude and also the experimental estimation of RRP sizes, as the initial phase is a measure of RRP depletion, whereas the linear phase is representative of ongoing RRP replenishment and immediate release of newly recruited vesicles (see Ma *et al.*, 2009). Our first observation was that, consistent with other preparations (Crowder *et al.*, 1999; Xu & Bajjalieh, 2001; Custer *et al.*, 2006; Chang & Sudhof, 2009), SV2A knockdown reduced stimuli-evoked transmitter release in cholinergic SCG synapses. Initial EPSP amplitudes in SV2A-siRNA-injected neurons were significantly attenuated compared with nsRNA-injected neurons (nsRNA: 17.9 ± 7.0 mV, $n = 10$ vs. SV2A-siRNA: 12.4 ± 1.6 mV, $n = 7$; $P < 0.05$, Student's two-sample *t*-test; Fig. 2C). The postsynaptic response can be modulated via the effects on RRP size or vesicle release probability. We investigated the effects of SV2A-siRNA on RRP size. In this regard, one major difference in studies delineating SV2A mechanisms is in reports regarding the differential effects of SV2 knockout on RRP size (Custer *et al.*, 2006; Chang & Sudhof, 2009). In our experiments, cumulative integrals of data sets were fitted with linear regressions to the steady-state replenishment phases and extrapolated to individual values at the zero time point (Fig. 2D and E). The linear component had similar slope values for nsRNA and SV2A-siRNA (nsRNA: 1.5 ± 0.5 mV/s, $n = 6$ vs. SV2A-siRNA: 1.3 ± 0.4 mV/s, $n = 5$; $P > 0.05$, Student's two-sample *t*-test), indicating that there was no replenishing defect following high-frequency action potential trains, as the steady-state replenishment rates were similar under SV2A knockdown. The reduced EPSP integral at the zero time point in SV2A-siRNA-treated (Fig. 2E) vs. nsRNA-treated SCGs (Fig. 2D) may suggest a reduction in RRP size due to SV2A knockdown. To quantify this effect, cumulative EPSP integrals were divided by the mean quantal EPSP integral to estimate the RRP size (Ma *et al.*, 2009). Here, a significant reduction in RRP size was seen (nsRNA: 79 ± 20 vesicles, $n = 6$ vs. SV2A-siRNA: 41 ± 27 vesicles; $P < 0.05$, Student's two-sample *t*-test; Fig. 2F). Together, these data suggest that presynaptic SV2A knockdown-induced decrease in EPSP amplitude is associated with the attenuation of RRP size, consistent with the availability of fewer release slots.

Presynaptic synaptic vesicle glycoprotein 2A knockdown increases paired-pulse depression and delays readily releasable pool recovery after depletion

We next investigated the consequences of SV2A knockdown upon the RRP in more detail. We applied a paired-pulse protocol whereby two successive action potentials were evoked presynaptically at varying interstimulus intervals (20–1000 ms) and the postsynaptic responses of the partner cell were recorded as EPSPs (Fig. 3A and B). These data, expressed as the paired-pulse ratio (PPR) (P2 : P1), showed that, for control nsRNA conditions, the PPR increased with interstimulus interval duration; these data are in good agreement with the PPR characteristics in control SCG synapses (Lu *et al.*, 2009; Ma *et al.*, 2009; Tanifuji *et al.*, 2013). The clear reduction in the PPR in the presence of SV2A-siRNA showed that synaptic depression was significantly increased in comparison to nsRNA at all interstimulus intervals measured (Fig. 3A and B). Whereas the

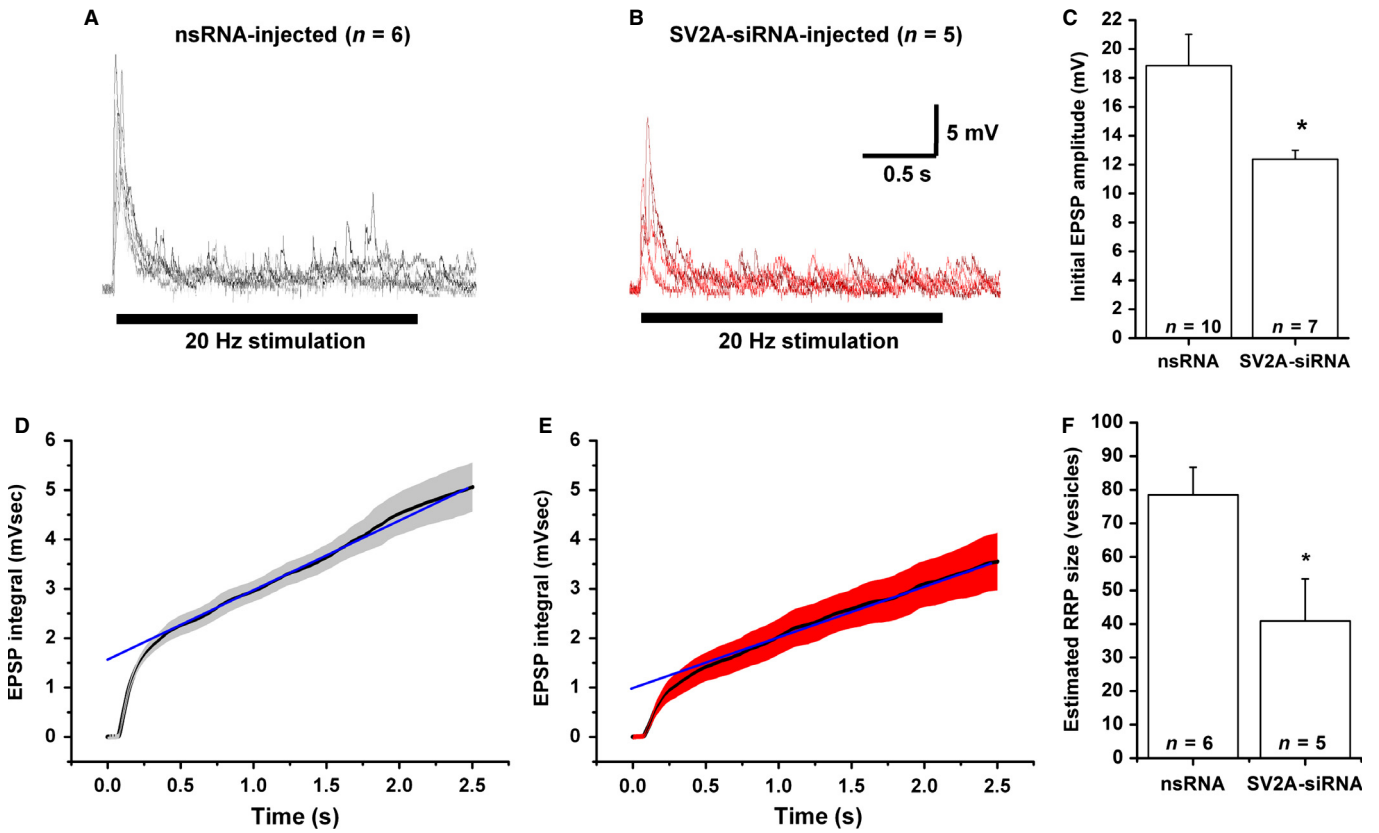

FIG. 2. Knockdown of SV2A reduces basal EPSP amplitudes and the size of the RRP in SCG synapses. Multi-peak EPSPs estimated by a train of action potentials (20 Hz, 2 s) for (A) nsRNA-injected and (B) SV2A-siRNA-injected neurons. (C) Initial EPSP amplitudes (mean + SEM) were significantly smaller in SV2A-siRNA-injected cells. Cumulative integrals of data in (A) and (B) plotted for (D) nsRNA and (E) SV2A-siRNA. The linear component was fitted with a linear regression y = mx + b between 0.5 and 2.0 s after onset of high-frequency stimulation (where m is the slope and b is the Y intercept), according to having an established stable steady-state response. Linear regression fits were extrapolated to time 0 and reflect a reduction in EPSP amplitude in SV2A-siRNA-injected cells. (F) The RRP size (number of vesicles in the RRP) was estimated by dividing cumulative EPSP integrals from D and E by the mean quantal EPSP integral (mean + SEM). RRP size was significantly reduced in SV2A-siRNA-injected cells. *$P < 0.05$, Student's two-sample *t*-test.

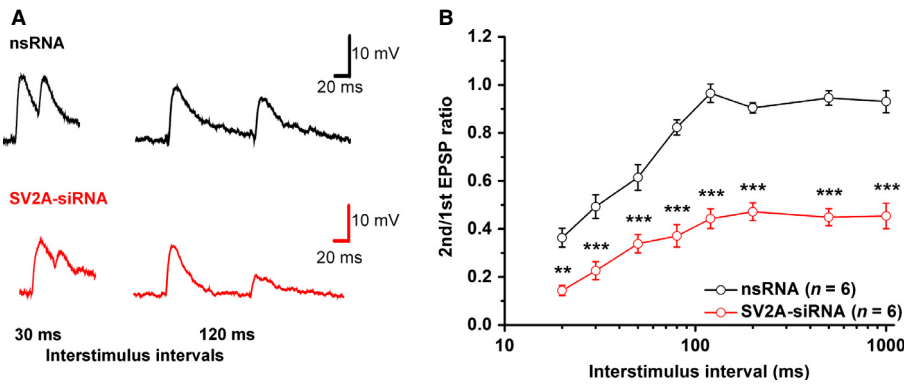

FIG. 3. Knockdown of SV2A increases synaptic depression in SCG synapses. (A) Representative traces of EPSPs elicited by two subsequently evoked action potentials at 30 and 120 ms interstimulus intervals (ISIs) in SCG neurons either injected with nsRNA (top) or SV2A-siRNA (bottom). (B) Ratios of the peak amplitude of the second EPSP over the first EPSP plotted against ISI (mean ± SEM). SV2A-siRNA caused an increase in magnitude of synaptic depression at all ISIs tested. **$P < 0.01$, ***$P < 0.001$, ANOVA followed by posthoc Bonferroni test.

PPRs of nsRNA-injected SCG synapses returned to baseline at an interstimulus interval of >100 ms, responses of SV2A siRNA-injected cells failed to recover, even at prolonged time intervals of up to 1 s, clearly indicating enhanced and deeper synaptic depression. These data suggest that, under normal conditions, SV2A aids rapid vesicular replenishment of the RRP and therefore acts to promote recovery from synaptic depression.

The above data demonstrate that SV2A regulates the RRP size and that changes to the RRP recovery kinetics may underlie the SV2A effects on stimuli-evoked transmitter release. Previous studies have reported that SV2-deficient central synapses had normal recovery kinetics following depletion of the RRP (Chang & Sudhof, 2009). However, another study reported a phenotype more consistent with our study and concluded that SV2A maintains the RRP

size and modulates the RRP refilling kinetics (Custer *et al.*, 2006). We have previously characterised the RRP recovery kinetics following pool depletion in SCG synapses (Lu *et al.*, 2009; Ma *et al.*, 2009); therefore, we next examined the dynamics of RRP refilling after depletion by monitoring the recovery of EPSP amplitudes (recorded at 1 Hz basal stimulation frequency) using a train of stimuli (5 Hz, 4 min) to clear release-ready vesicles from presynaptic terminals (Fig. 4A). SV2A knockdown caused an initial reduction in EPSP amplitude in comparison to nsRNA controls, consistent with the data above (Fig. 2C). Whereas the depletion phase followed a similar time course in both conditions, clear differences in the recovery phase were seen. We have previously demonstrated that, following RRP depletion, the synaptic vesicle pool in SCG synapses recovers via two phases, i.e. fast (complete by ~ 10 s) and slow (Lu

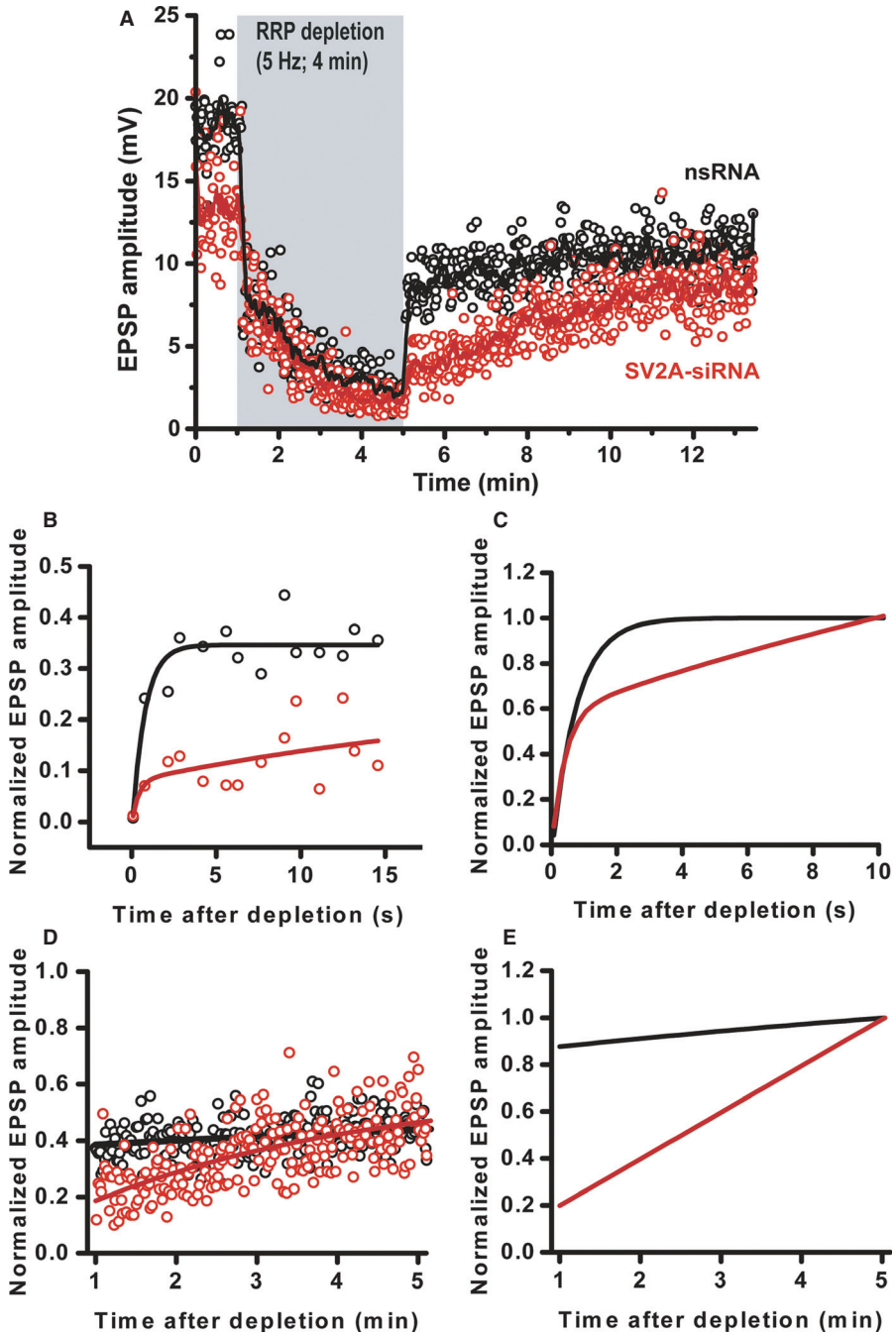

FIG. 4. Knockdown of SV2A delays RRP recovery after depletion in SCG synapses. (A) EPSP amplitudes recorded at 1 Hz basal stimulation frequency before and after a depleting stimulus (5 Hz, 4 min) either injected with nsRNA (black line) or SV2A-siRNA (red line). SV2A-siRNA caused a major depression in rapid replenishment phase with fast refilling kinetics remaining unchanged (inset). EPSP amplitudes normalised to the mean value prior to start of depletion, shown for individual time points postdepletion for (B) the fast recovery phase (0–10 s) and (D) the slow recovery phase (1–5 min). (C) Normalised recovery curves for the fast recovery phase were best fitted with a single exponential function fit to group data for nsRNA (black line: $\tau_{recovery}$ = 0.3 s), but required a triple exponential function for SV2A-siRNA (red line: $\tau_{recovery1}$ = 0.3 s, $\tau_{recovery2}$ = 26.0 s, $\tau_{recovery2}$ = 26.3 s). (E) Normalised recovery curves for the slow recovery phase were best fitted with a single exponential function fit to group data for nsRNA (black line: $\tau_{recovery}$ = 12.1 min) and SV2A-siRNA (red line: $\tau_{recovery1}$ = 3.5 min).

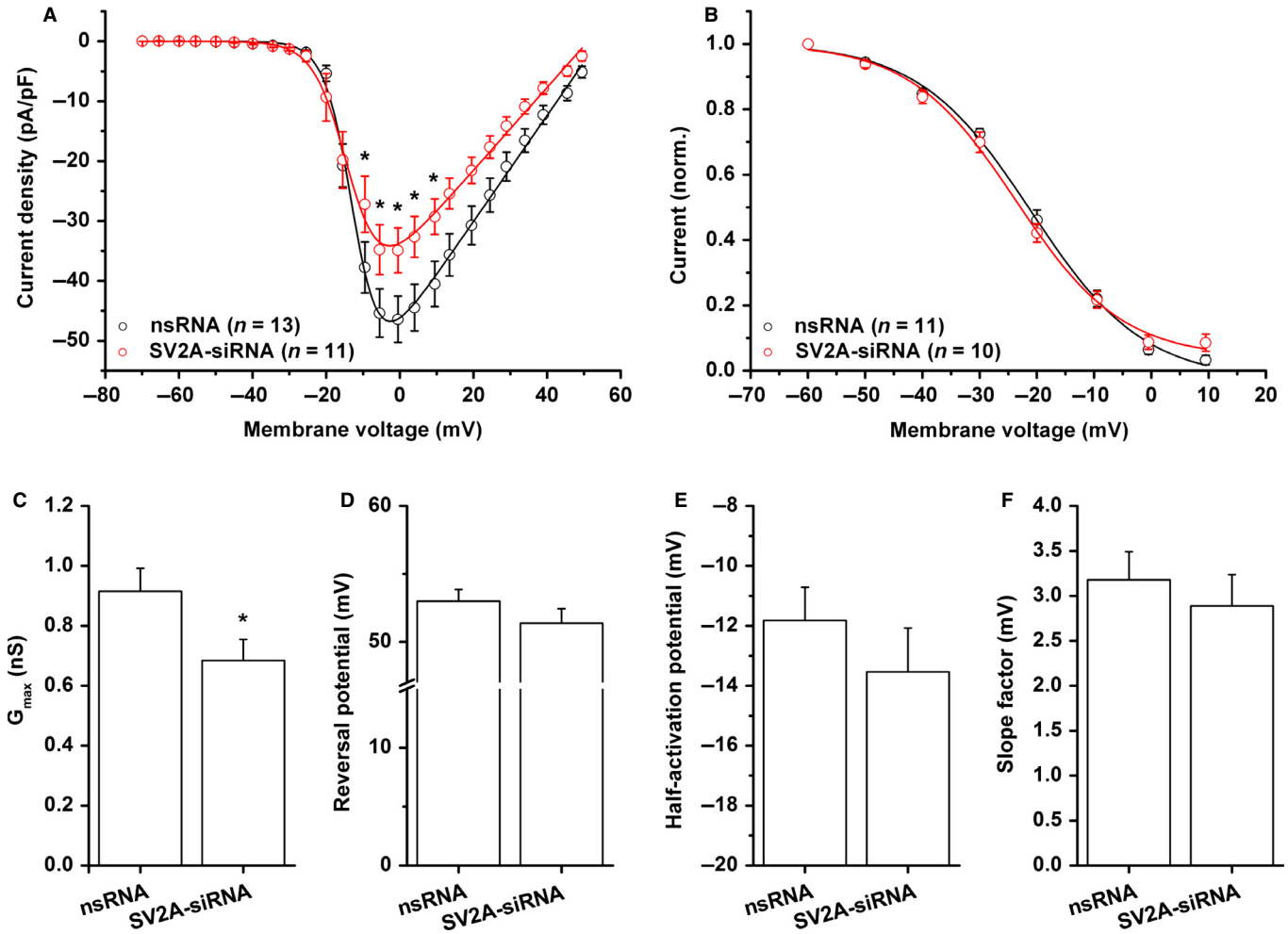

FIG. 5. Knockdown of SV2A impairs presynaptic VDCC function in SCG neurons. (A) Current–voltage relationships from SCG neurons injected with either nsRNA or SV2A-siRNA reveal a significant reduction in current density around peak values (*$P < 0.05$, repeated-measures ANOVA followed by posthoc Bonferroni test). (B) Steady-state inactivation data show similar voltage dependency of inactivation properties between the two groups. (C) The maximum conductance (G_{max}) of SV2A-siRNA-injected neurons is significantly reduced in comparison to the nsRNA group (*$P < 0.05$, two-sample Student's *t*-test). Other parameters, including (D) reversal potential, (E) half-activation potential and (F) slope factor remain unchanged after SV2A-siRNA-mediated knockdown. All data are mean ± SEM.

TABLE 1. Effects of SV2A-siRNA on I_{Ca} activation properties in SCG neurons

	Mean ± SEM		
Parameter	nsRNA (n = 13)	SV2A-siRNA (n = 11)	P-value
Maximum conductance (G_{max}) (nS)	0.92 ± 0.08	0.68 ± 0.07	0.04
Half-activation potential ($V_{0.5}$) (mV)	−11.8 ± 1.1	−13.5 ± 1.5	0.35
Slope factor (k) (mV)	3.2 ± 0.3	2.9 ± 0.4	0.54
Reversal potential (V_{rev}) (mV)	53.0 ± 0.9	51.4 ± 1.1	0.24

et al., 2009; Ma *et al.*, 2009; Tanifuji *et al.*, 2013). The rapid, initial phase of recovery is proposed to represent vesicle recruitment from the reserve pool (RP) and the slow component is proposed to indicate replenishment through endocytotic pathways. Here, the fast phase of RRP recovery was shown over 0-10 s (Fig. 4B and C) and the slow phase over 1–5 min (Fig. 4D and E). For control nsRNA, the RRP recovered with fast kinetics according to a single exponential fit to the fast recovery phase and with recovery complete by ~4 s (Fig. 4C). For SV2A-siRNA, the recovery of the EPSP amplitude was clearly attenuated during the fast phase, with the recovery rate fitted with a more complex triple exponential function (Fig. 4C). Continuously, the slow phase of recovery was also altered (Fig. 4D and E), suggesting that SV2A knockdown caused a delaying of RRP replenishment with vesicles from the RP during the fast phase and a bypassing of the RP during the slow phase. Overall, these findings strongly implicated a role for SV2A in maintaining correct RRP refilling in SCG synapses.

Synaptic vesicle glycoprotein 2A knockdown impairs presynaptic voltage-dependent Ca^{2+} channel current density in sympathetic neurons

Regulated exocytosis is highly dependent on precise presynaptic Ca^{2+} influx (Sudhof, 2004) and SV2A modulation of presynaptic

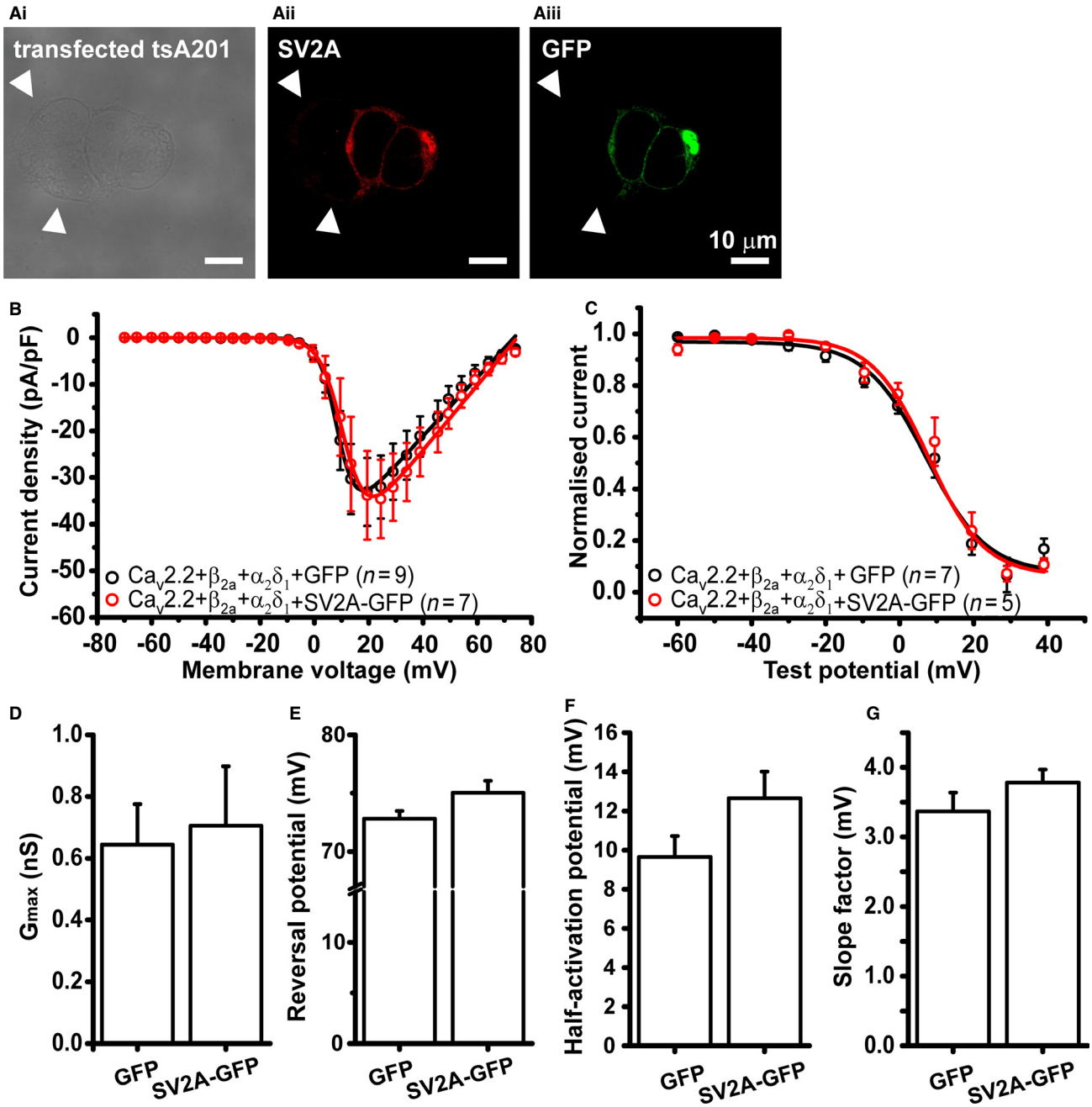

FIG. 6. Overexpression of SV2A does not alter $Ca_V2.2$ function in transfected tsA201 cells. (A) Transiently transfected tsA201 cells express SV2A-GFP in close proximity to the plasma membrane. Representative confocal section of a central plane through tsA201cells transfected with SV2A-GFP, with (Ai) transmitted light, (Aii) GFP and (Aiii) SV2A staining. Note the absence of SV2A immunoreactivity in the proximal non-transfected cells (indicated by arrowheads in A). SV2A plasma membrane localization was apparent; the large intracellular fluorescent signal probably represents the endoplasmatic reticulum/Golgi of the HEK cells. (B) Current–voltage relationships from tsA201 cells transiently transfected with $Ca_V2.2/\alpha_2\delta_1/\beta_{2a}$ and either GFP or SV2A-GFP showed no change in current density (P = 0.96; repeated-measures ANOVA). (C) Steady-state inactivation data were recorded from the same batch of cells as in B and show similar voltage dependency of inactivation properties. Parameters including (D) maximum conductance (G_{max}), (E) reversal potential, (F) half-activation potential and (G) slope factor remain unchanged between GFP-transfected and SV2A-GFP-transfected cells. All data are mean ± SEM.

VDCCs could contribute to the deficient secretory phenotype described here. Moreover, use of high-frequency action potential trains to deplete the RRP involves stimuli-induced Ca^{2+} entry into the presynaptic terminal, permitting the study of activity-dependent regulation of vesicle priming and replenishment (Stevens & Wesseling, 1998). Therefore, we examined the effects of SV2A knockdown on whole-cell I_{Ca} in isolated SCG neurons, measured using approximately physiological Ca^{2+} (2 mM), as the best available model of the presynapse. $Ca_V2.2$ channels underlie transmitter release at SCG synapses (Mochida *et al.*, 2003) and are the predominant VDCC isoform in somatic whole-cell recordings from these neurons (~85% of whole-cell I_{Ca}; remainder largely carried by L-type VDCCs) (Bucci *et al.*, 2011). In conditions in which L-type VDCCs were inhibited by 10 μM nifedipine, SCG neurons injected with SV2A-siRNA showed a ~25% reduction in peak Ca^{2+} current density in comparison to nsRNA-injected cells (Fig. 5A) and a corresponding

TABLE 2. Effects of GFP-SV2A on I_{Ca} in recombinant $Ca_V2.2/\alpha_2\delta_1/\beta_{2a}$ activation properties in tsA201 cells

	Mean ± SEM		
Parameter	GFP (n = 9)	GFP-SV2A (n = 6)	P-value
Maximum conductance (G_{max}) (nS)	0.64 ± 0.13	0.71 ± 0.19	0.79
Half-activation potential ($V_{0.5}$) (mV)	9.7 ± 1.1	12.6 ± 1.4	0.10
Slope factor (k) (mV)	3.4 ± 0.3	3.8 ± 0.2	0.28
Reversal potential (V_{rev}) (mV)	72.9 ± 0.7	75.0 ± 1.0	0.08

decrease in maximum conductance (g_{max}) (Fig. 5C; Table 1). There were no SV2A-siRNA-induced changes to other biophysical properties derived from current–voltage relationships (Fig. 5D–F; Table 1). There were also no alterations in steady-state inactivation parameters (Fig. 5B). These data are consistent with SV2A regulating Ca^{2+} influx through presynaptic VDCCs in SCG neurons without changing voltage-dependent activation and inactivation properties, in addition to maintaining the RRP.

Finally, we used a heterologous expression system to examine the effects of overexpressing SV2A-GFP on recombinant $Ca_V2.2/\alpha_2\delta_1/\beta_{2a}$ channels. Here, despite the expression of SV2A-GFP at or close to the plasma membrane (Fig. 6A), the voltage dependence of activation (Fig. 6B) and associated parameters (Fig. 6D–G; Table 2) were unchanged by SV2A-GFP. $Ca_V2.2/\alpha_2\delta_1/\beta_{2a}$ steady-state inactivation was also unaffected by SV2A-GFP (Fig. 6C). The demonstration that the modulation of SV2A expression affects VDCC current density in native neurons, but not recombinant channels in a non-neuronal expression system, may indicate that an, as yet unidentified, neuronal protein is necessary to mediate the SV2A–$Ca_V2.2$ interaction, as discussed more fully below.

Discussion

In this study, we investigated the unknown contribution of the synaptic vesicle protein SV2A to neurotransmission in peripheral SCG neurons. We used an siRNA strategy and injected directly into SCG synapses to reduce solely presynaptic SV2A levels. Our approach differs from previous studies using transgenic mouse models to reduce SV2A levels, which may potentially be confounded by accompanying compensatory and/or developmental changes (Crèvecœur *et al.*, 2013). Throughout, the siRNA experiments were controlled by an appropriate nsRNA; in this regard, the nsRNA construct produced control parameters, including EPSP amplitude, RRP size, overall vesicle count and synaptic depression characteristics, which were in good agreement with control data from our previous studies in SCG neurons (Krapivinsky *et al.*, 2006; Ma *et al.*, 2009; Tanifuji *et al.*, 2013; Mori *et al.*, 2014), suggesting that the injection of RNA had no detrimental effects *per se* on basal cell physiology in this experimental system (Ma & Mochida, 2007).

Synaptic vesicle glycoprotein 2A maintains normal neurotransmission by regulating readily releasable pool size in sympathetic neurons

We demonstrate that SV2A-siRNA-injected SCG neurons have abnormalities in stimuli-evoked neurotransmitter release, as previously shown for SV2-deficient central neurons (Crowder *et al.*, 1999; Janz *et al.*, 1999; Custer *et al.*, 2006; Chang & Sudhof, 2009), rod bipolar cells (Wan *et al.*, 2010) and adrenal chromaffin cells (Xu & Bajjalieh, 2001). Our results initially suggest the conservation of SV2A function on evoked release between peripheral and central neurons as well as neuroendocrine cells. In our experiments, two different stimulation protocols revealed an SV2A-siRNA-mediated reduction in EPSP amplitude, suggesting that SV2A is required to maintain regulated stimuli-evoked neurotransmission at SCG synapses. The SV2A-siRNA effects on multi-peak EPSPs evoked by high-frequency trains of action potentials suggest that the reduction in EPSP amplitude in the initial phase is mainly due to a reduction in RRP size. We provide evidence that SV2A knockdown may also increase the vesicular release probability in SCG neurons; in particular, and as discussed further below, we report a clear increase in synaptic depression, a phenomenon accompanied by increased release probability in SCG synapses (Ma *et al.*, 2009). Our data are in general agreement with those proposed by Custer *et al.* (2006), who similarly reported that SV2 regulates RRP size in hippocampal excitatory autapses. This group also reported a similar reduction in RRP size in SV2A-deficient adrenal chromaffin cells (Xu & Bajjalieh, 2001). Moreover, Wan *et al.* (2010) reported a secretory phenotype in SV2B-deficient rod bipolar cells characterised by a decrease in the number of rapidly releasing vesicles. Our data do, however, contrast with those from Chang & Sudhof (2009), who reported that SV2-deficient cortical neurons, despite similar reductions in stimuli-evoked transmission, have a normal RRP size. The reasons for these disparities may reflect the nature of the synapses investigated; Chang & Sudhof (2009) examined effects at cortical, glutamatergic synapses, whereas we investigate peripheral, cholinergic synapses. Related to this, glutamatergic and GABAergic terminals in the hippocampus preferentially express different SV2 isoforms (Gronborg *et al.*, 2010), which might influence synaptic release differentially, as reported in CA1 hippocampal neurons (Venkatesan *et al.*, 2012). Finally, the differential expression of other presynaptic proteins that associate with SV2 could potentially contribute to phenotypic variations within distinct cell populations.

Synaptic vesicle glycoprotein 2A promotes readily releasable pool refilling and recovery after depletion

We also investigated the effects of SV2A on synaptic plasticity. At SCG synapses, PPRs are dependent on the presynaptic Ca^{2+} channel subtype. Synaptic release at SCG synapses is almost exclusively mediated by $Ca_V2.2$ (Mochida *et al.*, 2003); release mediated by endogenous $Ca_V2.2$ is associated with persistent synaptic depression at physiological external Ca^{2+} concentrations (Lu *et al.*, 2009; Ma *et al.*, 2009; Tanifuji *et al.*, 2013). In the central nervous system, the major VDCC isoform is typically $Ca_V2.1$ (or a mixture of $Ca_V2.1$ and $Ca_V2.2$), thus, $Ca_V2.2$-dependent paired-pulse depression in SCG synapses is longer than is typically reported for central neurons. Here, SV2A knockdown increased paired-pulse depression at physiological Ca^{2+} concentrations. However, the synaptic response to an SV2 deficit appears to be highly dependent on the nature of the synapse investigated, e.g. SV2A or SV2A/B deletion was reported to cause an increase in paired-pulse facilitation in hippocampal autapses under similar conditions (Custer *et al.*, 2006). Here, our data are consistent with a facilitatory role for SV2A in the recovery from synaptic depression.

Following depletion of the RRP using a train of stimuli, EPSP amplitudes recovered more slowly in SV2A-siRNA-injected neurons than nsRNA-injected cells, consistent with the hypothesis that SV2A aids refilling of the RRP to maintain normal neurotransmission. Thus, the RRP size is smaller than control (Fig. 2), as indicated by the finding that the paired-pulse depression is enhanced (Fig. 3). RRP recovery from the depletion followed a fast and slow phase in

both nsRNA-injected and SV2A-siRNA-injected neurons (Fig. 4). Recovery curves illustrate the clearly attenuated EPSP amplitude in SV2A-siRNA-injected neurons during the fast phase, suggesting incomplete recovery in the fast phase, contributing to ~35% recovery with nsRNA and less than 10% recovery with siRNA. These results also suggest that the RP size is smaller after a train of stimuli with SV2A knockdown. SV2A deficits in the fast phase are also proposed to delay RRP replenishment from the RP and cause impaired, i.e. temporally delayed, Ca^{2+}-dependent long-term vesicle replenishment from the RP to the RRP following depletion (Mori *et al.*, 2014). It was also reported that SV2B deletion in rod bipolar cells caused a slowing in recovery of membrane capacitance in response to a train of stimuli, potentially reflecting a slowing in the rate of endocytosis (Wan *et al.*, 2010). These effects were proposed to occur secondarily to changes in Ca^{2+} signaling (see also Mori *et al.*, 2014). Overall, our data support a scenario whereby, in control conditions, empty release slots are filled rapidly after the cessation of high-frequency stimulation through vesicles from the recycling pool, whereas, under conditions of SV2A knockdown, this process takes longer and appears to be more reliant on slower endocytic pathways. In contrast to our findings that a major effect of SV2A is to promote RRP refilling, previous studies using similar depletion/recovery experimental paradigms in central neurons have reported differential SV2A effects on RRP recovery. Custer *et al.* (2006) reported that SV2-deficient hippocampal autapses exhibited a short-lived increase in RRP recovery in response to exhaustive (40 Hz for 5 min) stimuli-induced depletion, whereas Chang & Sudhof (2009) observed no differences in RRP recovery to depletion using milder (10 Hz for 10 s) stimuli in cortical neurons. As above, it appears that the SV2A effects on the RRP differ between synapses; moreover, such effects may also be influenced by the depletion protocols used. We have characterised the effects of several different presynaptic modulatory agents on the RRP recovery from depletion in SCG synapses (Lu *et al.*, 2009; Ma *et al.*, 2009). Using the same protocols here, we demonstrate that SV2A knockdown clearly slows RRP recovery in this preparation. Overall, we demonstrate that presynaptic SV2A knockdown is associated with a secretory phenotype, suggesting that SV2A acts to regulate stimuli-evoked transmission by maintaining the RRP and facilitating recovery from synaptic depression.

Synaptic vesicle glycoprotein 2A maintains presynaptic voltage-dependent Ca^{2+} channel current density in sympathetic neurons

The requirement for SV2A for normal neurotransmission might also involve effects on presynaptic VDCCs. For example, the observed RRP attenuation is characteristic of reduced Ca^{2+} influx through presynaptic VDCCs (Xu & Wu, 2005) and increased synaptic depression can be caused by decreased RRP size and altered replenishment and/or impaired VDCC function (Zucker & Regehr, 2002). In addition, the slowed recovery from RRP depletion seen is consistent with a reduction in presynaptic Ca^{2+} (Mori *et al.*, 2014). Here, we demonstrate, for the first time, that SV2A knockdown reduces whole-cell I_{Ca}. These data raise the possibility that the secretory phenotype occurs, at least partially, downstream of Ca^{2+} channel deficits. In our study, the SV2A-siRNA-mediated decrease in VDCC current density was not accompanied by any change to biophysical properties such as the voltage dependence of activation or steady-state inactivation. We have previously shown that the SV2A ligand, levetiracetam, attenuates the Ca^{2+} current density in SCG neurons without effects on the voltage dependence of activation and inactivation (Vogl *et al.*, 2012). Such data potentially reflect a pharmacological disruption of SV2A function by levetiracetam similar to that reported here for SV2A-siRNA. In this regard, it has been reported that levetiracetam modulates SV2A neuronal function (Nowack *et al.*, 2011) and that the antiepileptic efficacy of levetiracetam was reduced in heterozygous SV2A mice (Kaminski *et al.*, 2009).

Here, we were unable to demonstrate any effects of SV2A overexpression on recombinant $Ca_V2.2$ channels in HEK cells. Although HEK cells lack conventional synaptic vesicles, we propose that SV2A is targeted to transport vesicles resupplying plasma membrane proteins in non-neuronal cells (see Feany *et al.*, 1993). Previous studies suggest that correct SV2A glycosylation is maintained in HEK cells (Dong *et al.*, 2008), consistent with the SV2A HEK cell plasma membrane association shown here and by others (Peng *et al.*, 2011). Furthermore, the recombinant SV2A expressed in HEK cells was shown to retain the pharmacology towards small molecule ligands, indicating that the SV2A protein is correctly processed and folded in this cell system (Gillard *et al.*, 2006; Daniels *et al.*, 2013). Previous proteomic studies did not detect a direct physical link between isolated $Ca_V2.2$ and SV2A (Khanna *et al.*, 2007; Muller *et al.*, 2010), which may reflect this reported lack of direct SV2A effects on $Ca_V2.2$. However, the clear phenotype seen in native SCG neurons might indicate that an intermediate linker protein, present in SCG neurons and necessary to translate the SV2A-dependent modulation of $Ca_V2.2$, is absent in HEK cells. Candidate molecules here include synaptotagmin, which has been shown to interact with both the synprint site of the intracellular $Ca_V2.2$ II–III linker (Sheng *et al.*, 1997) and the N-terminus of SV2A in a Ca^{2+}-dependent manner (Schivell *et al.*, 1996; Yao *et al.*, 2010). Moreover, this interaction was shown to regulate transmitter release in SCG synapses (Schivell *et al.*, 2005). Another candidate is AP-2, which also interacts with SV2A, synaptotagmin and the $Ca_V2.2$ synprint site (Haucke & De Camilli, 1999; Watanabe *et al.*, 2010).

Previous reports have suggested presynaptic Ca^{2+} accumulation due to perturbation of SV2 expression (Chang & Sudhof, 2009). However, other groups have disputed this hypothesis (Custer *et al.*, 2006). Here, the reduced VDCC current density seen following SV2A knockdown might support the Ca^{2+} accumulation hypothesis at SCG synapses, as increased $[Ca]_i$ could facilitate Ca^{2+}-dependent VDCC inactivation. However, we report no changes to steady-state inactivation and the dramatic increase in synaptic depression seen in our paired-pulse experiments argues against this idea, as elevated presynaptic Ca^{2+} has been shown to accelerate recovery from synaptic depression (Fioravante & Regehr, 2011). In the future, it will be of interest to determine if a linker between SV2A and $Ca_V2.2$ is indeed required and, also, if the reported direct SV2A interaction with $Ca_V2.1$ (the major VDCC subunit in central synapses cf. the predominant role of $Ca_V2.2$ in peripheral synapses) has effects on VDCC function in central synapses that are similar to those reported here.

Function of synaptic vesicle glycoprotein 2A in sympathetic neurons

Our data provide compelling evidence that SV2A is required for regulated neurotransmission at peripheral cholinergic synapses. We demonstrate a requirement for SV2A for normal neurotransmission at SCG synapses, suggesting a broad conservation of SV2A function between central and peripheral synapses. We propose that SV2A knockdown leads to a deficient secretory phenotype that can be explained by a combination of altered vesicle recruitment to the RRP and aberrant VDCC function. Our findings not only support

SV2A acting as an important factor to establish RRP size, as proposed previously in central synapses, but also suggest that SV2A has a previously undescribed Ca^{2+} channel phenotype, acting as a positive modulator of presynaptic VDCCs.

Supporting Information

Additional supporting information can be found in the online version of this article:
Fig. S1. Evaluation of multiple siRNAs to assess SV2A knock-down efficiency in stable Rn-SV2A HEK293T cells.

Acknowledgements

The authors would like to thank Dr James Foster, Dr Giovanna Bucci, Camille Soubrane and Michinori Mori for excellent technical support. Part of this work was supported by a Japan Society for Promotion of Science award to C.V.

Abbreviations

DMEM, dulbecco's modified eagle's medium; EPSP, excitatory postsynaptic potential; GFP, green fluorescent protein; nsRNA, non-silencing RNA; PPR, paired-pulse ratio; RP, reserve pool; RRP, readily releasable pool; SCG, superior cervical ganglion; siRNA, small interference RNA; SV, synaptic vesicle glycoprotein; VDCC, voltage-dependent Ca^{2+} channel.

References

Bajjalieh, S.M., Peterson, K., Shinghal, R. & Scheller, R.H. (1992) SV2, a brain synaptic vesicle protein homologous to bacterial transporters. *Science*, **257**, 1271–1273.

Bucci, G., Mochida, S. & Stephens, G.J. (2011) Inhibition of synaptic transmission and G protein modulation by synthetic $Ca_V2.2$ Ca^{2+} channel peptides. *J. Physiol.-London*, **589**, 3085–3101.

Buckley, K. & Kelly, R.B. (1985) Identification of a transmembrane glycoprotein specific for secretory vesicles of neural and endocrine cells. *J. Cell Biol.*, **100**, 1284–1294.

Chang, W.P. & Sudhof, T.C. (2009) SV2 renders primed synaptic vesicles competent for Ca^{2+}-induced exocytosis. *J. Neurosci.*, **29**, 883–897.

Crèvecœur, J., Foerch, P., Doupagne, M., Thielen, C., Vandenplas, C., Moonen, G., Deprez, M. & Rogister, B. (2013) Expression of SV2 isoforms during rodent brain development. *BMC Neurosci.*, **14**, 87.

Crowder, K.M., Gunther, J.M., Jones, T.A., Hale, B.D., Zhang, H.Z., Peterson, M.R., Scheller, R.H., Chavkin, C. & Bajjalieh, S.M. (1999) Abnormal neurotransmission in mice lacking synaptic vesicle protein 2A (SV2A). *Proc. Natl. Acad. Sci. USA*, **96**, 15268–15273.

Custer, K.L., Austin, N.S., Sullivan, J.M. & Bajjalieh, S.M. (2006) Synaptic vesicle protein 2 enhances release probability at quiescent synapses. *J. Neurosci.*, **26**, 1303–1313.

Daniels, V., Wood, M., Leclercq, K., Kaminski, R.M. & Gillard, M. (2013) Modulation of the conformational state of the SV2A protein by an allosteric mechanism as evidenced by ligand binding assays. *Brit. J. Pharmacol.*, **169**, 1091–1101.

De Smedt, T., Raedt, R., Vonck, K. & Boon, P. (2007) Levetiracetam: the profile of a novel anticonvulsant drug-part I: preclinical data. *CNS Drug Rev.*, **13**, 43–56.

Dong, M., Yeh, F., Tepp, W.H., Dean, C., Johnson, E.A., Janz, R. & Chapman, E.R. (2006) SV2 is the protein receptor for botulinum neurotoxin A. *Science*, **312**, 592–596.

Dong, M., Liu, H., Tepp, W.H., Johnson, E.A., Janz, R. & Chapman, E.R. (2008) Glycosylated SV2A and SV2B mediate the entry of botulinum neurotoxin E into neurons. *Mol. Biol. Cell*, **19**, 5226–5237.

Feany, M.B., Lee, S., Edwards, R.H. & Buckley, K.M. (1992) The synaptic vesicle protein SV2 is a novel type of transmembrane transporter. *Cell*, **70**, 861–867.

Feany, M.B., Yee, A.G., Delvy, M.L. & Buckley, K.M. (1993) The synaptic vesicle proteins SV2, synaptotagmin and synaptophysin are sorted to separate cellular compartments in CHO fibroblasts. *J. Cell Biol.*, **123**, 575–584.

Fioravante, D. & Regehr, W.G. (2011) Short-term forms of presynaptic plasticity. *Curr. Opin. Neurobiol.*, **21**, 269–274.

Gillard, M., Chatelain, P. & Fuks, B. (2006) Binding characteristics of levetiracetam to synaptic vesicle protein 2A (SV2A) in human brain and in CHO cells expressing the human recombinant protein. *Eur. J. Pharmacol.*, **536**, 102–108.

Gronborg, M., Pavlos, N.J., Brunk, I., Chua, J.J., Munster-Wandowski, A., Riedel, D., Ahnert-Hilger, G., Urlaub, H. & Jahn, R. (2010) Quantitative comparison of glutamatergic and GABAergic synaptic vesicles unveils selectivity for few proteins including MAL2, a novel synaptic vesicle protein. *J. Neurosci.*, **30**, 2–12.

Haucke, V. & De Camilli, P. (1999) AP-2 recruitment to synaptotagmin stimulated by tyrosine-based endocytic motifs. *Science*, **285**, 1268–1271.

Iacovitti, L., Joh, T.H., Park, D.H. & Bunge, R.P. (1981) Dual expression of neurotransmitter synthesis in cultured autonomic neurons. *J. Neurosci.*, **1**, 685–690.

Iezzi, M., Theander, S., Janz, R., Loze, C. & Wollheim, C.B. (2005) SV2A and SV2C are not vesicular Ca^{2+} transporters but control glucose-evoked granule recruitment. *J. Cell Sci.*, **118**, 5647–5660.

Janz, R., Goda, Y., Geppert, M., Missler, M. & Sudhof, T.C. (1999) SV2A and SV2B function as redundant Ca^{2+} regulators in neurotransmitter release. *Neuron*, **24**, 1003–1016.

Kaminski, R.M., Gillard, M., Leclercq, K., Hanon, E., Lorent, G., Dassesse, D., Matagne, A. & Klitgaard, H. (2009) Proepileptic phenotype of SV2A-deficient mice is associated with reduced anticonvulsant efficacy of levetiracetam. *Epilepsia*, **50**, 1729–1740.

Khanna, R., Li, Q., Bewersdorf, J. & Stanley, E.F. (2007) The presynaptic $Ca_V2.2$ channel-transmitter release site core complex. *Eur. J. Neurosci.*, **26**, 547–559.

de Kok, J.B., Ruers, T.J., van Muijen, G.N., van Bokhoven, A., Willems, H.L. & Swinkels, D.W. (2000) Real-time quantification of human telomerase reverse transcriptase mRNA in tumors and healthy tissues. *Clin. Chem.*, **46**, 313–318.

Krapivinsky, G., Mochida, S., Krapivinsky, L., Cibulsky, S.M. & Clapham, D.E. (2006) The TRPM7 ion channel functions in cholinergic synaptic vesicles and affects transmitter release. *Neuron*, **52**, 485–496.

Lu, W., Ma, H., Sheng, Z.H. & Mochida, S. (2009) Dynamin and activity regulate synaptic vesicle recycling in sympathetic neurons. *J. Biol. Chem.*, **284**, 1930–1937.

Lynch, B.A., Lambeng, N., Nocka, K., Kensel-Hammes, P., Bajjalieh, S.M., Matagne, A. & Fuks, B. (2004) The synaptic vesicle protein SV2A is the binding site for the antiepileptic drug levetiracetam. *Proc. Natl. Acad. Sci. USA*, **101**, 9861–9866.

Ma, H. & Mochida, S. (2007) A cholinergic model synapse to elucidate protein function at presynatic terminals. *Neurosci. Res.*, **57**, 491–498.

Ma, H., Cai, Q., Lu, W., Sheng, Z.H. & Mochida, S. (2009) KIF5B motor adaptor syntabulin maintains synaptic transmission in sympathetic neurons. *J. Neurosci.*, **29**, 13019–13029.

Mendoza-Torreblanca, J.G., Vanoye-Carlo, A., Phillips-Farfán, B.V., Carmona-Aparicio, L. & Gómez-Lira, G. (2013) Synaptic vesicle protein 2A: basic facts and role in synaptic function. *Eur. J. Neurosci.*, **38**, 3529–3539.

Mochida, S. (1995) Role of myosin in neurotransmitter release: functional studies at synapses formed in culture. *J. Physiol. Paris*, **89**, 83–94.

Mochida, S., Westenbroek, R.E., Yokoyama, C.T., Itoh, K. & Catterall, W.A. (2003) Subtype-selective reconstitution of synaptic transmission in sympathetic ganglion neurons by expression of exogenous calcium channels. *Proc. Natl. Acad. Sci. USA*, **100**, 2813–2818.

Mori, M., Tanifuji, S. & Mochida, S. (2014) Kinetic organization of Ca2 + signals that regulate synaptic release efficacy in sympathetic neurons. *Mol. Pharmacol.*, **86**, 297–305.

Muller, C.S., Haupt, A., Bildl, W., Schindler, J., Knaus, H.G., Meissner, M., Rammner, B., Striessnig, J., Flockerzi, V., Fakler, B. & Schulte, U. (2010) Quantitative proteomics of the Ca_V2 channel nano-environments in the mammalian brain. *Proc. Natl. Acad. Sci. USA*, **107**, 14950–14957.

Nowack, A., Malarkey, E.B., Yao, J., Bleckert, A., Hill, J. & Bajjalieh, S.M. (2011) Levetiracetam reverses synaptic deficits produced by overexpression of SV2A. *PLoS One*, **6**, e29560.

Peng, L., Tepp, W.H., Johnson, E.A. & Dong, M. (2011) Botulinum neurotoxin D uses synaptic vesicle protein SV2 and gangliosides as receptors. *PLoS Pathog.*, **7**, e1002008.

Schivell, A.E., Batchelor, R.H. & Bajjalieh, S.M. (1996) Isoform-specific, calcium-regulated interaction of the synaptic vesicle proteins SV2 and synaptotagmin. *J. Biol. Chem.*, **271**, 27770–27775.

Schivell, A.E., Mochida, S., Kensel-Hammes, P., Custer, K.L. & Bajjalieh, S.M. (2005) SV2A and SV2C contain a unique synaptotagmin-binding site. *Mol. Cell. Neurosci.*, **29**, 56–64.

Schneider, C.A., Rasband, W.S. & Eliceiri, K.W. (2012) NIH Image to ImageJ: 25 years of image analysis. *Nat. Methods*, **9**, 671–675.

Sheng, Z.H., Yokoyama, C.T. & Catterall, W.A. (1997) Interaction of the synprint site of N-type Ca^{2+} channels with the C2B domain of synaptotagmin I. *Proc. Natl. Acad. Sci. USA*, **94**, 5405–5410.

Stephens, G.J. & Mochida, S. (2005) G protein βγ subunits mediate presynaptic inhibition of transmitter release from rat superior cervical ganglion neurones in culture. *J. Physiol.-London*, **563**, 765–776.

Stevens, C.F. & Wesseling, J.F. (1998) Activity-dependent modulation of the rate at which synaptic vesicles become available to undergo exocytosis. *Neuron*, **21**, 415–424.

Sudhof, T.C. (2004) The synaptic vesicle cycle. *Annu. Rev. Neurosci.*, **27**, 509–547.

Tanifuji, S., Funakoshi-Tago, M., Ueda, F., Kasahara, T. & Mochida, S. (2013) Dynamin isoforms decode action potential firing for synaptic vesicle recycling. *J. Biol. Chem.*, **288**, 19050–19059.

Venkatesan, K., Alix, P., Marquet, A., Doupagne, M., Niespodziany, I., Rogister, B. & Seutin, V. (2012) Altered balance between excitatory and inhibitory inputs onto CA1 pyramidal neurons from SV2A-deficient but not SV2B-deficient mice. *J. Neurosci. Res.*, **90**, 2317–2327.

Vogl, C., Mochida, S., Wolff, C., Whalley, B.J. & Stephens, G.J. (2012) The synaptic vesicle glycoprotein 2A ligand levetiracetam inhibits presynaptic Ca^{2+} channels through an intracellular pathway. *Mol. Pharmacol.*, **82**, 199–208.

Wan, Q.F., Zhou, Z.Y., Thakur, P., Vila, A., Sherry, D.M., Janz, R. & Heidelberger, R. (2010) SV2 acts via presynaptic calcium to regulate neurotransmitter release. *Neuron*, **66**, 884–895.

Watanabe, H., Yamashita, T., Saitoh, N., Kiyonaka, S., Iwamatsu, A., Campbell, K.P., Mori, Y. & Takahashi, T. (2010) Involvement of Ca^{2+} channel synprint site in synaptic vesicle endocytosis. *J. Neurosci.*, **30**, 655–660.

Xu, T. & Bajjalieh, S.M. (2001) SV2 modulates the size of the readily releasable pool of secretory vesicles. *Nat. Cell Biol.*, **3**, 691–698.

Xu, J. & Wu, L.G. (2005) The decrease in the presynaptic calcium current is a major cause of short-term depression at a calyx-type synapse. *Neuron*, **46**, 633–645.

Yao, J., Nowack, A., Kensel-Hammes, P., Gardner, R.G. & Bajjalieh, S.M. (2010) Cotrafficking of SV2 and synaptotagmin at the synapse. *J. Neurosci.*, **30**, 5569–5578.

Yeh, F.L., Dong, M., Yao, J., Tepp, W.H., Lin, G., Johnson, E.A. & Chapman, E.R. (2010) SV2 mediates entry of tetanus neurotoxin into central neurons. *PLoS Pathog.*, **6**, e1001207.

Zucker, R.S. & Regehr, W.G. (2002) Short-term synaptic plasticity. *Annu. Rev. Physiol.*, **64**, 355–405.